Journal of Electrochemistry

Volume 24
Issue 6 *Special Issue in Honor of Professor Baolian Yi on His 80th Birthday*

2018-12-28

Acid Treated Carbon as Anodic Electrocatalysts toward Direct Ascorbic Acid Alkaline Membrane Fuel Cells

He-mu CHEN

Chen-xi QIU

Yuan-yuan CONG

Hui-yuan LIU

Zi-hui ZHAI

Yu-jiang SONG
State Key Laboratory of Fine Chemicals, School of Chemical Engineering, Dalian University of Technology, Dalian 116024, China;, yjsong@dlut.edu.cn

Recommended Citation

He-mu CHEN, Chen-xi QIU, Yuan-yuan CONG, Hui-yuan LIU, Zi-hui ZHAI, Yu-jiang SONG. Acid Treated Carbon as Anodic Electrocatalysts toward Direct Ascorbic Acid Alkaline Membrane Fuel Cells[J]. *Journal of Electrochemistry*, 2018 , 24(6): 748-756.
DOI: 10.13208/j.electrochem.180844
Available at: https://jelectrochem.xmu.edu.cn/journal/vol24/iss6/16

DOI: 10.13208/j.electrochem.180844 **Artical ID**:1006-3471(2018)06-0748-09
Cite this: *J. Electrochem.* **2018**, *24*(6): 748-756 **Http**://electrochem.xmu.edu.cn

Acid Treated Carbon as Anodic Electrocatalysts toward Direct Ascorbic Acid Alkaline Membrane Fuel Cells

CHEN He-mu[1], QIU Chen-xi[1], CONG Yuan-yuan[1], LIU Hui-yuan[1,2], ZHAI Zi-hui[1], SONG Yu-jiang[1*]

(1. *State Key Laboratory of Fine Chemicals, School of Chemical Engineering, Dalian University of Technology, Dalian* 116024, *China*; 2. *Dalian Institute of Chemical Physics, Chinese Academy of Sciences, Dalian* 116023, *China*)

Abstract: In order to improve the hydrophilicity and electrocatalytic activity, commercial carbon black (BP 2000) was subjected to acid treatment to obtain acid-treated carbon (ATC). The generation of rich oxygen-containing groups on the surface of the ATC was proved by X-ray photoelectron spectra (XPS), Fourier transform-infra red spectra (FTIR), thermogravimetric analysis (TG) and contact angle measurement. UV-vis spectra were firstly recorded to calculate activation energy (*E*a) of ascorbic acid (AA) chemical oxidation in alkaline conditions by oxygen in air and the *E*a value was determined to be 37.1 kJ·mol^{-1}. Additionally, electrochemical impedance spectra (EIS) were used to evaluate unprecedented $Ea_{electrochem}$ of ATC as electrocatalysts toward ascorbic acid (AA) oxidation in alkaline media. The $Ea_{electrochem}$ values of electrochemical oxidation in alkaline membrane electrode assembly (MEA) setup of a single cell without and with ATC as the anodic electrocatalysts were calculated to be 34.5 and 26.5 kJ·mol^{-1}, respectively. The diminished $Ea_{electrochem}$ suggests that ATC does function as an effective anodic electrocatalyst. Furthermore, the ATC was applied in direct ascorbic acid alkaline membrane fuel cell (DAAFC) for the first time. We optimized a series of parameters for the fabrication of MEAs including catalyst coated membrane (CCM) or catalyst coated gas diffusion layer membrane (CDM), loading of anodic electrocatalyst, and ionomer content in the electrocatalyst slurry. It turned out that the CCM with the ATC loading of 0.5 mg·cm^{-2} and 25wt% ionomer reached a high power density of 18.5 mW·cm^{-2}, which is higher than that of using PtRu/C as anodic electrocatalyst (less than 5.0 mW·cm^{-2}). In addition, the DAAFC fed with 15 mL·min^{-1} of the fuel containing 0.5 mol·L^{-1} AA and 1 mol·L^{-1} NaOH aq. could stably hold a power density at 4 mW·cm^{-2} for 25 min.

Key words: direct ascorbic acid alkaline membrane fuel cells; carbon; anodic electrocatalysts; activation energy; acid treatment

CLC Number: O646 **Document Code**: A

Since liquid fuel like methanol bears apparent advantages in safety, storage, and production compared with gas counterparts[1], direct liquid fuel polymer electrolyte membrane fuel cells have attracted a great deal of attention. However, fuel crossover and toxicity have somehow hindered practical applications[1]. In this regard, researchers have been seeking the substitute of methanol for decades and found molecules (ethanol[2] and formic acid[3]) may serve as reasonably good candidates. In particular, biomass based fuel molecules such as glycerol[4], glucose[5], lignin[6], urea[7], and ascorbic acid (Vitamin C, AA) are becoming the focus because of the abundance, safety, carbon neutral recyclability[5]. It is necessary to point out that AA has two hydroxyl groups in the molecular structure and can be readily oxidized[8], thus a high power density is highly expected.

In the field of the anodic electrocatalysts toward electrochemical oxidation reaction of AA, noble metals[9-10], polymer[11-12], photoelectric materials[13], and carbon[14-16] have been explored. Carbon shows a much better activity than other electrocatalysts and the

Received: 2018-08-27, Revised: 2018-09-25 *Corresponding author, Tel: (86-411)84986485, E-mail: yjsong@dlut.edu.cn

highest power density of 18 mW·cm^{-2} was attained in acidic operating conditions of DAAFCs[17]. Previous studies showed that ATC could more efficiently catalyze electrochemical oxidation of AA in acidic and neutral conditions owning to the change in surface groups after acid treatment[18-19].

AA has been proved to be oxidized more easily in alkaline media than in acidic media[8]. Although the mechanism of AA electrooxidation in alkaline media is still elusive, the generation of ascorbate and diketoguloconate represents AA deep degradation[20]. This well explains a higher open circuit potential (0.7 ~ 0.9 V) in alkaline membrane fuel cells than that in acidic membrane ones (0.5 ~ 0.6 V)[17, 21]. Some noble metals have been applied as anodic electrocatalysts in DAAFCs[21-22], however, carbon electrocatalysts have not been reported prior to this study.

In this study, acid treatment was applied to commercial carbon black that was utilized as an anodic electrocatalyst in DAAFC. The *E*a of AA (electro)-hemical oxidation in alkaline conditions was investigated by UV-vis and EIS. For the first time, the electrocatalytic effect of ATC on AA electrooxidation in alkaline media was clearly identified. Furthermore, the MEA fabrication method, the anodic electrocatalyst loading, and the ionomer content were optimized so that a high power density of 18.5 mW·cm^{-2} was achieved. In addition, the stability of the single cell was briefly assessed.

1 Experimental

1.1 Chemicals and Materials

Ultrapure water (18.2 MΩ·cm at 25 °C, Synergy UV, France) was used throughout in this research (simplified as water in the following unless otherwise stated). AT-1 Anion exchange membrane (40 μm) and alkaline ionomer suspension (2wt%, Shanghai Hephas Energy Corporation) were applied in DAAFCs. Black Pearls 2000 (BP2000, Cabot) was suspended in 3 mol·L^{-1} HCl aq. for 1 h at 30 °C and 4 mol·L^{-1} HNO_3 aq. for 1 h at 80 °C under stirring. Next, the carbon was washed by copious amount of water until the filtrate reached neutral pH. Finally, the carbon was dried in an oven at 65 °C under vacuum for future use and labeled as ATC. Anodic gas diffusion layer (0.19 mm in thickness, TORAY TGP-H-060) was soaked in 5 mol·L^{-1} HNO_3 aq. for 6 h at 80 °C, and washed and dried as above.

1.2 MEA Fabrication and Single Cell Tests

Anodic electrocatalyst layer was prepared by spraying electrocatalyst ink (2 mg·mL^{-1}, V_{Water}:$V_{Ethanol}$ = 1:9[23-24], the ionomer content ranged from 10wt% to 50wt%) onto AT-1 membrane (CCM method) or onto gas diffusion (CDM) with a loading of 0 ~ 0.5 mg·cm^{-2}. Similarly, cathodic electrocatalyst (Pt/C, 60wt%, Johnson-Matthey, loading 0.4 mg_{Pt}·cm^{-2}) layer was prepared on the other side of the membrane by using an ink[25-26] of 2 mg·mL^{-1} (V_{Water}:$V_{Ethanol}$:$V_{Ionomer}$ = 1:9:0.25). The obtained MEAs were immersed in 1 mol·L^{-1} NaOH aq. for 48 h and briefly rinsed with water. In the following, the MEAs were sandwiched between untreated (cathode) and treated (anode) gas diffusion layers by hot pressing at 40 °C and 6 MPa for 2 min. The MEAs were assembled in fuel cell hardware (FX201-2D, Kunshan Sunlaite New Energy Technology Co. Ltd, P. R. China) with a 4 cm^2 active geometric area. Single cell tests were all performed at 75 °C unless otherwise stated on a self-made fuel cell test system with an electronic load (PLZ1004WH, Kikusui). Liquid fuel containing 0.5 mol·L^{-1} AA and 1 mol·L^{-1} NaOH aqueous solution (Sinopharm Chemical Reagent Co. Ltd) was continuously pumped by a peristaltic pump to the anode side (15 mL·min^{-1}) and humidified oxygen (100% RH) was supplied to the cathode side (200 mL·min^{-1}).

1.3 Characterizations

EIS of DAAFC were recorded in pseudo-potentiostatic mode on AUTOLAB electrochemical workstation (PGSTA302N, Metrohm). XPS were measured on an ESCALAB™ 250Xi photoelectron spectrometer (Thermo Fisher) with Al K_α X-ray as an excitation source. FTIR and UV-vis adsorption spectra were recorded on FTIR spectrometer (6700, Thermo Fisher) and UV spectrophotometer (S600, Analytic Jena), respectively. TG curves were performed on TGA (Q600, TA Instruments). The surface hydrophilicity of carbon was examined on contact angle measuring

instrument (DSA100, KRUSS).

2 Results and Discussion

2.1 Acid Treatment of Carbon

Acid treatment of carbon has been shown to be an effective method for the improvement of electrocatalytic activity toward AA oxidation in acidic[18] and pH neutral[19] conditions. A similar phenomenon may also exist in alkaline conditions, and thus we treated BP2000 with acid (see details in experimental). A major difference between ATC and the pristine BP2000 is the quantity of oxygen-containing groups (OCG) on the carbon surface. According to XPS (Fig. 1A), high-resolution C1s spectra can be de-convoluted into C-C (284.6 eV), C-O (286.2 eV), C=O (287.0 eV), and COOH (288.2 eV) peaks[27]. The peak areas of C-O and COOH increase from 6.18% and 1.49% to 9.95% and 3.04%, respectively, after the acid treatment. So, the enhanced OCG of ATC originates from the formation of C-O and COOH groups. This result was also proved by FTIR in Fig. 1B. Compared with the BP2000, the appearance of C=O (1680-1850 cm^{-1}) and C-O (1100-1300 cm^{-1})[28] in the ATC verifies the existence of more OCG on the ATC surface. Since more OCG are formed after the acid treatment, the ATC should adsorb more water. This is confirmed by TG analysis as shown in Fig. 1C that the ATC adsorbs 15wt% more water than the BP2000. Similarly, we also treated gas diffusion layer with acid. The contact angle of the gas diffusion layer after acid treatment decreases from 140.2° to 76.5° (Fig. 1D). As a result, the hydrophilicity of the gas diffusion layer is improved, and thus the diffusion of AA aq. might become much easier[29].

2.2 Evaluations of Activation Energy

UV-vis measurements were conducted to calculate the *E*a of chemical oxidation of AA in air in basic solution. When the molar ratio of AA/OH^- was 1/2, the main absorption peak centered at about 267

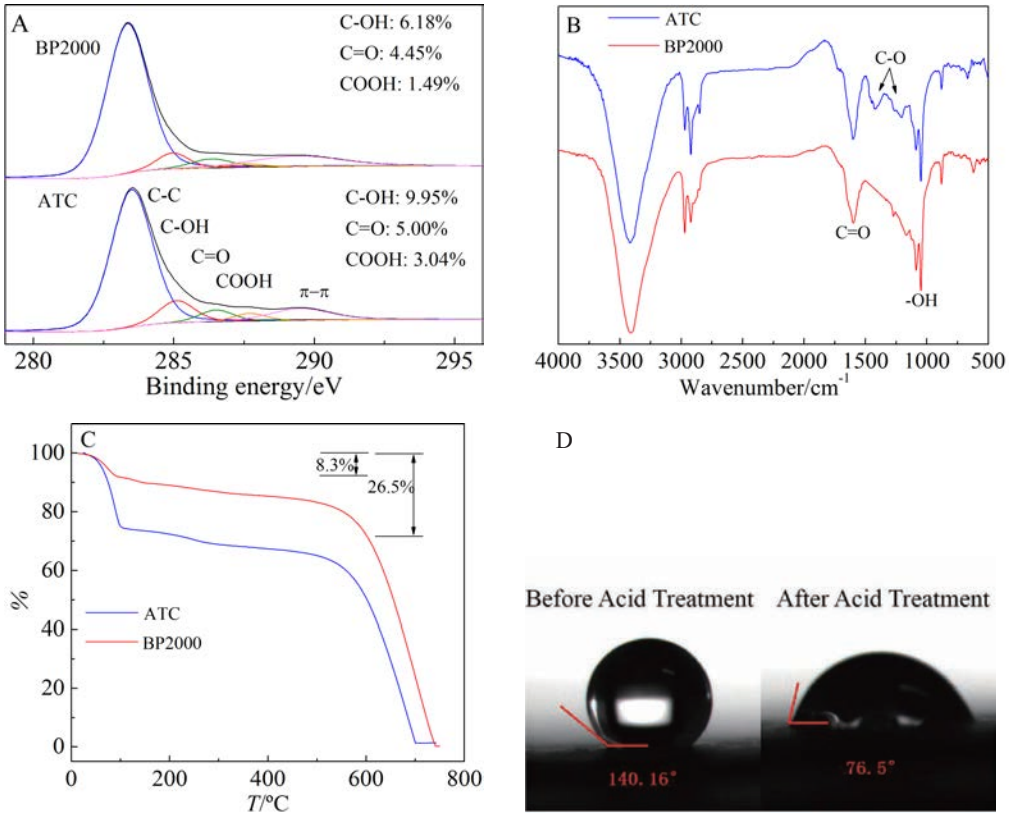

Fig. 1 (A) High-resolution C1s spectra of XPS, (B) FTIR spectra (all spectra have been taken after making pellets using KBr), (C) TG curves (all samples had absorbed water for 24 h in water-saturated air before the tests, and the ramping rate was 10 °C·min^{-1}) of the BP2000 and the ATC, (D) Contact angle analysis of gas diffusion layers before and after acid treatment.

nm (Fig. 2) can be assigned to de-protonated AA (deprived of one hydrogen atom, AH^-) that is the main species in an alkaline condition[30]. In Fig. 2A-E, the absorption maxima (A) decline to zero at five temperatures (15 °C, 25 °C, 35 °C, 45 °C, 55 °C) in a few hours, indicative of the chemical oxidation of AA by air. The obtained A values are linearly correlated to the concentration of AH^- (c_{AH^-}). According to the first order reaction model ($\ln(c_{AH^-}/c_{AH^-0}) = -kt$), the reaction rate ($k$) was fitted at different temperatures. Furthermore, the Ea value was calculated to be 37.1 kJ·mol^{-1} for the first time by linear fitting Arrhenius Formula ($\ln(k) = \ln(A) - Ea/RT$).

The $Ea_{electrochem}$ for AA electrooxidation in a single cell of DAAFCs was calculated based on EIS[31-33]. Since in the low-frequency region, the mass transfer is mainly limited by Warburg diffusion[17], the charge transfer resistance in the high-frequency region was analyzed in order to determine the value of the charge transfer resistance (R_{ct}). Given the fact that AA electrooxidation is too complicated to accurately analyze each reaction step, simplification is needed for the

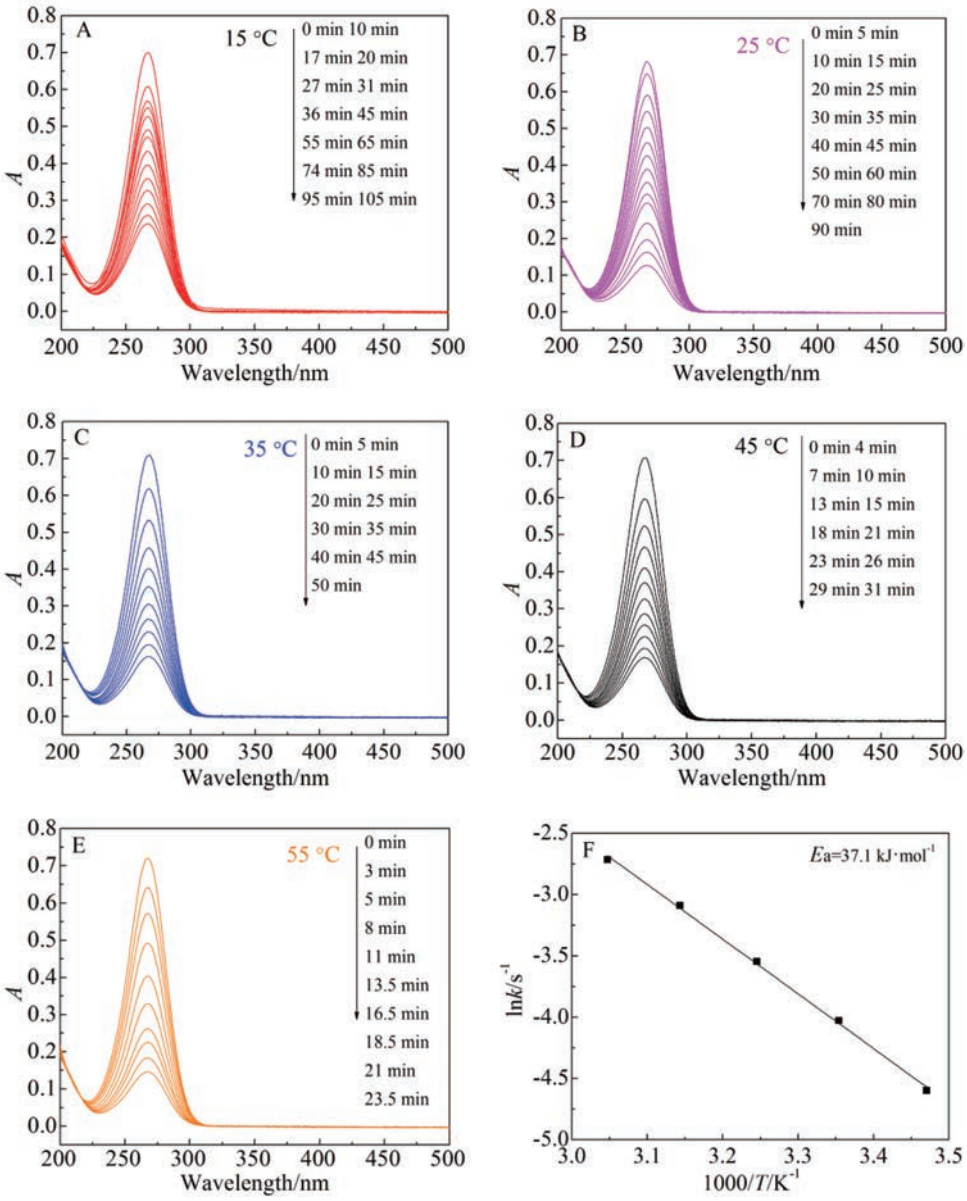

Fig. 2 UV-vis spectra of AA chemical oxidation in alkaline media at 15 ℃ (A), 25 ℃ (B), 35 ℃ (C), 45 ℃ (D), and 55 ℃ (E), and the fitting plot (F) of activation energy with a quartz cuvette of 1 cm path-length.

calculation of R_{ct}. As shown in Fig. 3A-B, curves were fitted in semicircles of which the diameter corresponds to the value of R_{ct}. Similar to the Ea calculation, Ea$_{electrochem}$ values with and without ATC as the anodic electrocatalyst were calculated by linear fitting to be 26.5 and 34.5 kJ·mol^{-1}, respectively, as shown in Fig. 3C. Ea$_{electrochem}$ with ATC decreases more than 30% as compared with Ea, verifying the expected electrocatalytic activity of ATC toward AA oxidation in alkaline condition. For the case of no ATC was used in the single cell of DAAFCs, the electrocatalytic activity of acid treated gas diffusion layer should contribute to the slight decrease in Ea, which is also displayed in Fig. 4D.

2.3 Single Cell Performance Enhancement of DAAFCs

The power density for the single cell of DAAFCs fabricated with the pristine BP2000 was 11.0 mW·cm^{-2}, lower than that (15.5 mW·cm^{-2}) of fabricated with the ATC as shown in Fig. 4A. The main difference between ATC and BP2000 is the quantity of OCG, which was identified by Fig. 1. Because the AA is negatively charged in the solution and the OCG makes the carbon surface positively charged, the increment of the OCG may be beneficial to the adsorption of negatively charged AA onto the surface of the ATC[18]. The OCG may also enhance its affinity towards the solvated electrolyte and electroactive species through electrostatic forces[17]. Similarly, the OCG on the carbon surface decreases the contact angle of gas diffusion layers and makes it more hydrophilic (Fig. 1D), and thus the diffusion of AA aq. might become much easier, which may also contribute to the performance improvement of DAAFCs.

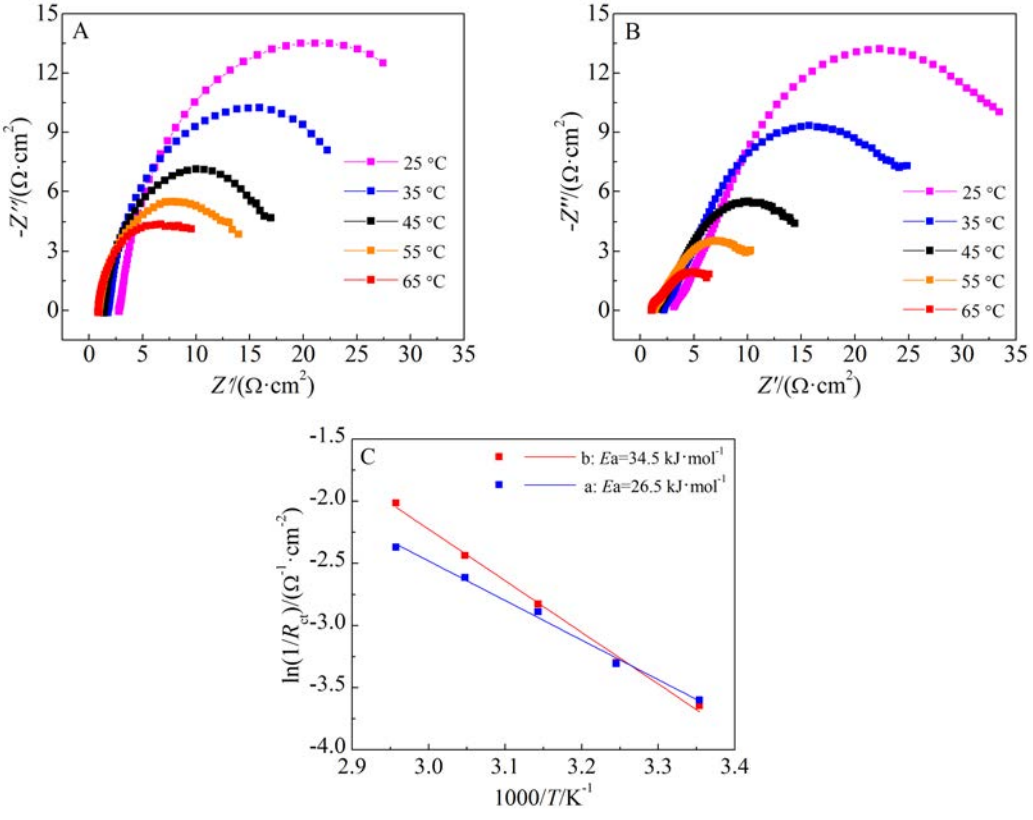

Fig. 3 Nyquist plots of single cells of DAAFCs fabricated with (A) and without (B) the ATC as anodic electrocatalyst at open circuit potential for different temperatures. All MEAs in single cells were performed on a house-made fuel cell test system. Liquid fuel containing 0.5 mol·L^{-1} AA and 1 mol·L^{-1} NaOH aqueous solution was continuously pumped by a peristaltic pump to the anode side (15 mL·min^{-1}) and humidified oxygen (100% RH) was supplied to the cathode side (200 mL·min^{-1}). (C) Fitting polts of activation energy based on (A) and (B).

Carbon materials have been previously identified to function as anodic electrocatalysts superior to noble metals toward AA oxidation in acidic[14] and neutral[19] conditions. In this study, we demonstrated that the ATC performs better than PtRu/C that usually serves as the anodic electrocatalyst toward AA oxidation in anion exchange membrane fuel cells. As shown in Fig. 4B, the power density of the single cell fabricated

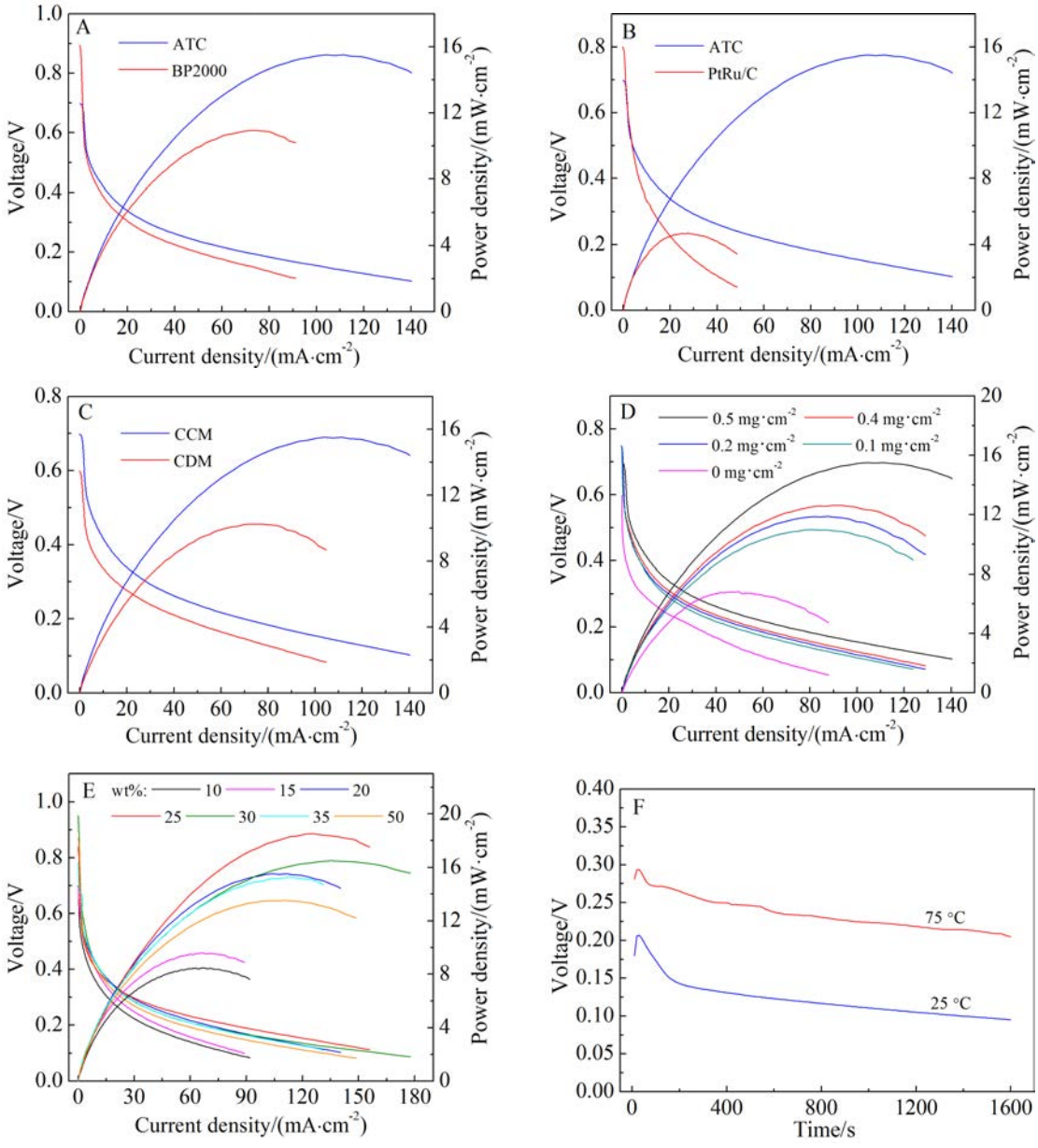

Fig. 4 Polarization and power density curves of MEAs fabricated differently: (A) CCM using BP2000 and ATC at a loading of 0.5 mg·cm^{-2} and 20wt% ionomer; (B) CCM using ATC and PtRu/C (60wt%, Johnson-Matthey) as the anodic electrocatalyst at a loading of 0.5 mg·cm^{-2} and 20wt% ionomer content; (C) CCM and CDM of 0.5 mg·cm^{-2} ATC loading with 20wt% ionomer content; (D) CCM of 0, 0.1, 0.2, 0.4, 0.5 mg·cm^{-2} ATC with 20wt% ionomer; (E) CCM of 0.5 mg·cm^{-2} ATC loading with 10wt%, 15wt%, 20wt%, 25wt%, 30wt%, 35wt%, 50wt% ionomer. (F) Voltage-Time curves for the single cell of DAAFCs at 75 and 25 °C with a constant current density of 20 mA·cm^{-2} and a 15 mL·min^{-1} liquid fuel solution circulation. All MEAs were evaluated on a self-made fuel cell test system. Liquid fuel containing 0.5 mol·L^{-1} AA and 1 mol·L^{-1} NaOH aqueous solution was continuously pumped by a peristaltic pump to the anode side (15 mL·min^{-1}) and humidified oxygen (100% RH) was supplied to the cathode side (200 mL·min^{-1}).

with PtRu/C is less than 5 mW·cm^{-2}, much lower that of the ATC (15.5 mW·cm^{-2}).

Though the single cell performance of the ATC was improved by acid treatment, the optimization in other aspects is still necessary to further enhance the DAAFCs performance. The MEA fabrication method can influence the performance of DAAFCs as shown in Fig. 4C. At the loading of 0.5 mg·cm^{-2}, the DAAFC fabricated with CDM shows a power density of 10.0 mW·cm^{-2} inferior to that of CCM (15.5 mW·cm^{-2}). As a result, the CCM approach has been adopted in the following paragraph.

Furthermore, the increase of the ATC loading has a positive effect on the performance of DAAFCs. As shown in Fig. 4D, the ideal loading of the ATC turned out to be 0.5 mg·cm^{-2}. A higher ATC loading causes the falling off of the ATC from the membrane. It is worth to point out that the power density of DAAFCs remains at 7.0 mW·cm^{-2} for the case at zero ATC loading, indicative of the electrocatalytic effect of acid treated gas diffusion layer to AA electrooxidation[17].

The ionomer content in the slurry of the ATC was also investigated. The optimal content of ionomer seems to differ from other studies possibly due to the special hydrophilicity of the ATC[10]. As shown in Fig. 4E, when the ionomer content is less than 25wt%, the single cell power density increases from 8.4 to 18.5 mW·cm^{-2} with more ionomer contents. Considering the adhesive function of ionomer in binding MEA tightly, in certain range, the lack of ionomer may cause unstable adhesion and possible falling off of ATC. As the ionomer content increases to over 25 wt%, the electrical conductivity of the ATC, and the contact between AA and carbon may be disturbed. As a result, the power density of DAAFCs decreases with the continuous increases of ionomer content to over 25wt%. The optimum ionomer content appears to be 25wt% with a power density of 18.5 mW·cm^{-2}.

Finally, the stability of DAAFCs was briefly investigated. The variation in the cell voltage of DAAFC at a current density of 20 mA·cm^{-2} with the elapsed time is shown in Fig. 4F. The power density declined to 4 mW·cm^{-2} in 25 min at 75 °C with the decrease of the voltage of DAAFC (Power density = Voltage · Current density). Furthermore, the stability test was also conducted at 25 °C and the power density dropped to 2 mW·cm^{-2} in 25 min. The attenuation of the power density may be caused by the chemical oxidation of AA and electrochemical consumption, as evidenced by the darkening of the AA fuel[8].

3 Conclusions

After acid treatment, the enriched OCG on the carbon surface can improve the electrocatalytic activity toward alkaline electrochemical AA oxidation. The *E*a values in air, and $Ea_{electrochem}$ values without and with the ATC as an anodic electrocatalyst were calculated to be 37.1, 34.5 and 26.5 kJ·mol^{-1}, respectively, verifying the electrocatalytic effect of the ATC for the first time in the alkaline conditions. The MEA fabricated by CCM with a loading of 0.5 mg·cm^{-2} and 25wt% ionomer content reaches a high power density of 18.5 mW·cm^{-2}. The stability test reveals that the single cell of DAAFCs can basically be operated stably.

Acknowledgements

This study was supported by National Key Research & Development Program of China (Gran No. 2016YFB0101307), National Natural Science Fund of China (Grant Nos. 21003114, 21103163, 21306188, 21373211, and 21306187), Liaoning BaiQianWan Talents Program (Grant No. 201519), Program for Liaoning Excellent Talents in University (Grant No. LR201514), Dalian Excellent Young Scientific and Technological Talents (Grant No. 2015R006).

References:

[1] Ma L(马亮), Cai W W(蔡卫卫), Zhang J(张晶), et al. Optimization of membrane electrode assembly in air-breathing direct methanol fuel cell[J]. Journal of Electrochemsitry (电化学), 2010, 16(2): 131-136.

[2] Hong Y H, Zhou Z Y, Zhan M, et al. Liquid-inlet online electrochemical mass spectrometry for the in operando monitoring of direct ethanol fuel cells[J]. Electrochemistry Communications, 2018, 87: 91-95.

[3] Liu D, Xie M, Wang C, et al. Pd-Ag alloy hollow nanostructures with interatomic charge polarization for en-

hanced electrocatalytic formic acid oxidation[J]. Nano Research, 2016, 9(6): 1590-1599.

[4] Benipal N, Qi J, Liu Q, et al. Carbon nanotube supported PdAg nanoparticles for electrocatalytic oxidation of glycerol in anion exchange membrane fuel cells[J]. Applied Catalysis B: Environmental, 2017, 210: 121-130.

[5] Cosnier S, Le Goff A, Holzinger M. Towards glucose biofuel cells implanted in human body for powering artificial organs: Review[J]. Electrochemistry Communications, 2014, 38: 19-23.

[6] Liu W, Mu W, Deng Y L. High-performance liquid-catalyst fuel cell for direct biomass-into-electricity conversion [J]. Angewandte Chemie International Edition, 2014, 53 (49): 13558-13562.

[7] Senthilkumar N, Gnana kumar G, Manthiram A. 3D hierarchical core-shell nanostructured arrays on carbon fibers as catalysts for direct urea fuel cells[J]. Advanced Energy Materials, 2018, 8(6): 1702207.

[8] Nováková L, Solich P, Solichová D. HPLC methods for simultaneous determination of ascorbic and dehydroascorbic acids[J]. TrAC Trends in Analytical Chemistry, 2008, 27(10): 942-958..

[9] Fujiwara N, Yasuda K, Ioroi T, et al. Direct polymer electrolyte fuel cells using L-ascorbic acid as a fuel[J]. Electrochemical and Solid-State Letters, 2003, 6(12): A257.

[10] Fujiwara N, Yamazaki S I, Siroma Z, et al. L-Ascorbic acid as an alternative fuel for direct oxidation fuel cells [J]. Journal of Power Sources, 2007, 167(1): 32-38.

[11] Mondal S K, Raman R K, Shukla A K, et al. Electrooxidation of ascorbic acid on polyaniline and its implications to fuel cells[J]. Journal of Power Sources, 2005, 145(1): 16-20.

[12] Homma T, Kondo M, Kuwahara T, et al. Immobilization of acid phosphatase on a polyaniline/poly(acrylic acid) composite film for use as the anode of a fuel cell driven with L-ascorbic acid 2-phosphate[J]. Polymer Journal, 2012, 44(11): 1117-1122.

[13] Li X D, Huang M G, Huang B, et al. Fabrication and catalytic properties of highly ordered single-walled carbon nanotube arrays coated with photoelectro-polymerized bisphenol A films for visible-light-enhanced ascorbate fuel cells[J]. Journal of Electroanalytical Chemistry, 2017, 803: 117-124.

[14] Fujiwara N, Yamazaki S, Siroma Z, et al. Direct oxidation of l-ascorbic acid on a carbon black electrode in acidic media and polymer electrolyte fuel cells[J]. Electrochemistry Communications, 2006, 8(5): 720-724.

[15] Mogi H, Fukushi Y, Koide S, et al. A flexible ascorbic acid fuel cell with a microchannel fabricated using MEMS techniques[M]. Journal of Physics: Conference Series, 2013, 476: 012065.

[16] Hoshi K, Muramatsu K, Sumi H, et al. Miniaturized ascorbic acid fuel cells with flexible electrodes made of graphene-coated carbon fiber cloth[J]. Japanese Journal of Applied Physics, 2016, 55(4): 04EC11.

[17] Uhm S, Choi J, Chung S T, et al. Electrochemically oxidized carbon anode in direct l-ascorbic acid fuel cells[J]. Electrochimica Acta, 2007, 53(4): 1731-1736.

[18] Choun M, Lee H J, Lee J. Positively charged carbon electrocatalyst for enhanced power performance of L-ascorbic acid fuel cells[J]. Journal of Energy Chemistry, 2016, 25(5): 793-797.

[19] Sathe B R. A scalable and facile synthesis of carbon nanospheres as a metal free electrocatalyst for oxidation of l-ascorbic acid: Alternate fuel for direct oxidation fuel cells[J]. Journal of Electroanalytical Chemistry, 2017, 799: 609-616.

[20] Deutsch J C. Dehydroascorbic acid[J]. Journal of Chromatography A, 2000, 881(1): 299-307.

[21] Muneeb O, Do E, Tran T, et al. A direct ascorbate fuel cell with an anion exchange membrane[J]. Journal of Power Sources, 2017, 351: 74-78.

[22] Majari Kasmaee L, Gobal F. A preliminary study of the electro-oxidation of l-ascorbic acid on polycrystalline silver in alkaline solution[J]. Journal of Power Sources, 2010, 195(1): 165-169.

[23] Yao R(姚瑞), Song Y J(宋玉江), Li H Q(李焕巧), et al. Preparation parameters optimization and electrocatalytic properties of supported Au nanoparticles[J]. Journal of Electrochemistry(电化学), 2016, 22(2): 147-156.

[24] Cong Y Y, Yi B L, Song Y J. Hydrogen oxidation reaction in alkaline media: From mechanism to recent electrocatalysts[J]. Nano Energy, 2018, 44: 288-303.

[25] Li J, Liu H Y, Lv Y, et al. Influence of counter electrode material during accelerated durability test of non-precious metal electrocatalysts in acidic medium[J]. Chinese Journal of Catalysis, 2016, 37(7): 1109-1118.

[26] Bai Y Z, Yi B L, Li J, et al. A high performance non-noble metal electrocatalyst for the oxygen reduction reaction derived from a metal organic framework[J]. Chinese Journal of Catalysis, 2016, 37(7): 1127-1133.

[27] Naseh M V, Khodadadi A A, Mortazavi Y, et al. Fast and clean functionalization of carbon nanotubes by dielectric barrier discharge plasma in air compared to acid treatment[J]. Carbon, 2010, 48(5): 1369-1379.

[28] Pinchas S, Laulicht I. Infrared spectra of labelled compounds[M]. London: Academic Press, 1971.

[29] Tan L S(谭力盛), Pan J(潘婧), Li Y(李瑶), et al. Influ-

ence of electrode hydrophobicity on performance of alkaline polymer electrolyte fuel cells[J]. Journal of Electrochemsitry(电化学), 2013, 19(3): 199-203.

[30] Berg R W. Investigation of *L*(+)-ascorbic acid with Raman spectroscopy in visible and UV light[J]. Applied Spectroscopy Reviews, 2014, 50(3): 193-239.

[31] Yan J B, Zhao Z, Shang L, et al. Co-synthesized Y-stabilized Bi_2O_3 and Sr-substituted $LaMnO_3$ composite anode for high performance solid oxide electrolysis cell[J]. Journal of Power Sources, 2016, 319: 124-130.

[32] Shang L, Wu W M, Zhao Z, et al. Oxygen-reduction reaction on preferred oriented $Gd_{0.1}Ce_{0.9}O_{2-\delta}$ films[J]. The Journal of Physical Chemistry C, 2018, 122(15): 8396-8405.

[33] Lee C G. Temperature effect on the electrode reactions in a molten carbonate fuel cell[J]. Journal of Electroanalytical Chemistry, 2018, 810: 48-54.

酸处理的碳作为阳极电催化剂用于直接抗坏血酸碱性膜燃料电池

陈禾木[1],邱晨曦[1],丛媛媛[1],刘会园[1,2],翟梓会[1],宋玉江[1*]

(1.大连理工大学,精细化工国家重点实验室 & 电化学工程实验室,化工学院,辽宁 大连,116024;
2. 中国科学院大连化物所,辽宁 大连,116023)

摘要: 为改善电催化活性和亲水性,作者对商业碳黑(BP2000)进行了酸处理,获得了酸处理碳(ATC). 通过 X 光电子能谱、红外光谱、热重和接触角测试的表征方法证明了酸处理在碳表面产生了丰富的含氧基团. 本文首次利用紫外可见光谱测试了碱性条件抗坏血酸(AA)在空气中的化学氧化活化能,结果为 37.1 kJ·mol^{-1}. 另外,利用交流阻抗谱对碱性条件下 ATC 作为电催化剂时 AA 的氧化反应的活化能进行了评价. 碱性条件下,AA 在单电池中有无 ATC 电催化剂层条件下的活化能分别为 26.5 和 34.5 kJ·mol^{-1}, 活化能的降低表明 ATC 是一种有效的阳极电催化剂. 作者将 ATC 应用于直接碱性膜 AA 燃料电池(DAAFCs)作为阳极电催化剂,并且对 DAAFC 中一系列参数进行了优化,包括催化剂在膜(CCM)或气体扩散层(CDM)上的喷涂方法、阳极电催化剂的载量、阳极电催化剂中碱性聚合物的比例. 结果表明, 采用 CCM 的膜电极制备方法、0.5 mg·cm^{-2} 的 ATC 载量、25wt%的碱性聚合物添加比例时,DAAFCs 单池的功率密度可达 18.5 mW·cm^{-2},远高于使用商品 PtRu/C(5 mW·cm^{-2})做阳极电催化剂的单池. 在寿命测试中,使用溶解于 1 mol·L^{-1} NaOH 水溶液中的 0.5 mol·L^{-1} AA 作为燃料(流速 15 mL·min^{-1}),DAAFCs 单池的功率密度可以在 25 min 内维持在 4 mW·cm^{-2} 以上(75 °C).

关键词: 直接碱性抗坏血酸燃料电池;碳;阳极电催化剂;活化能;酸处理